ISIJ International, Vol. 46 (2006), No. 11, pp. 1610–1617

Quantitative Estimation of Coupling Phenomenon between Reduction and Gasification on the Facing Pair of Iron Oxide and Graphite

Yoshiaki KASHIWAYA,[1] Motomichi KANBE[2] and Kuniyoshi ISHII[3]

1) Graduate School of Engineering, Hokkaido University, Kita-ku, Kita 13-jo, Nishi 3-chome, Sapporo 060-8628 Japan. E-mail: Yoshiaki@eng.hokudai.ac.jp 2) Formerly Student of Master course, Graduate School of Engineering, Hokkaido University. Now at Sumitomo Metal Co.Ltd. 3) Professor Emeritus of Hokkaido University. Now at Advisor of JFE Steel Co. Ltd., Kawasaki-cho, Chuo-ku, Chiba 260-0835 Japan.

(*Received on July 5, 2006; accepted on August 25, 2006*)

In previous study, the analysis of simultaneous reaction between the reduction reaction and the gasification reaction in a facing pair was performed. The definition of the coupling phenomenon was proposed. It was found that the starting temperature of gasification decreased from 900 to 600°C in the facing pair under CO_2 atmosphere.

In present study, the quantitative estimation of coupling phenomenon between reduction and gasification was carried out with modified experimental setup, in which all reaction gas (Ar–30%CO_2) could be passed through the space of facing pair of iron oxide (hematite) and graphite. Reduction reaction was promoted by the gasification reaction occurring in the opposite surface and the extent of reduction reaction was obtained as a function of the distance.

In the shortest distance, 0.5 mm, the CO_2 flow rate increased in the outlet gas, which meant that the reduction reaction was promoted and CO_2 gas reproduced during experiment.

The ratio of RDR (reduction rate) to RCS (gasification rate) increased until 0.5 mm from 1.5 mm, which was the distance of facing pair of hematite and graphite.

KEY WORDS: coupling reaction; coupling phenomenon; iron ore reduction; gasification; mechanism of reduction and gasification.

1. Introduction

In the case of composite pellet consisted of iron ore and carbonaceous material, since the relatively high reaction rate and low reaction temperature can be obtained for the ironmaking process,[1] many new processes (FASTMET, Iron Dynamics, INMETCO, ITmk3, Hi-Qip and so on) including a dust processing have developed and competed in the field of the next generation's ironmaking. In addition, such a circumstance will be intensified by the rack of energy and resources which are resulted from the rapid growth of NICs (Newly Industrializing Countries).

Although the actual reaction mechanisms in the composite pellet were complicated, at least two mechanisms in terms of reduction reaction will exist and can be illustrated in **Fig. 1**. One is the reaction resulted from the direct contact between iron oxide and solid carbon (Fig. 1(a)), which might be predominant in an initial stage of the reduction of composite pellet. The other is the coupling phenomenon occurring after the separation of the reaction interface (Fig. 1(b)).

In the previous study,[2] thermodynamic definition on the coupling phenomenon was presented and the existence of the coupling phenomenon between reduction of iron oxide (1) and carbon gasification reaction (2) was demonstrated.

$$FeO_x + CO = FeO_{x-1} + CO_2 \quad \text{.....(1)}$$

$$C + CO_2 = 2CO \quad \text{.....(2)}$$

The relationship between the affinity 'A' and the change of free energy 'ΔG' on the reaction 'i' is expressed as follow:

$$A_i = -\Delta G_i = -(\Delta G_i^\circ + RT \ln Kp) \quad \text{.....(3)}$$

The condition of the coupling phenomenon between the reduction and the gasification is expressed in Eq. (4)[2,3];

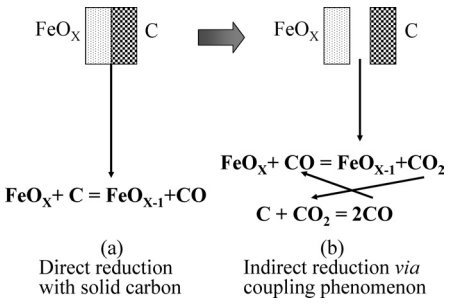

Fig. 1. Illustration of reaction mechanism in the carbon composite between iron oxide and carbon.

$$A_R v_R + A_G v_G > 0 \quad (A_R v_R < 0 \text{ and } A_G v_G > 0) \text{ .....(4)}$$

where A_R and A_G (J/mol), which are defined by Eqs. (5) and (6), are chemical affinity of reduction and gasification, respectively. v_R and v_G (mol/s) are the rate of reduction and gasification, respectively.

$$A_R = -\Delta G_R = -\left(\Delta G_R^\circ + RT \ln \frac{P_{CO_2}}{P_{CO}}\right) \text{ .....(5)}$$

$$A_G = -\Delta G_G = -\left(\Delta G_G^\circ + RT \ln \frac{P_{CO}^2}{P_{CO_2}}\right) \text{ .....(6)}$$

Where ΔG_R° and ΔG_G° are the standard free energy of reduction and gasification reaction, respectively. The ΔG_R° and ΔG_G° can be calculated using thermodynamic data.[4)]

The rates of reduction (RDR) and gasification (RCS) can be obtained experimentally through the oxygen balance (Eq. (7)) and carbon balance (Eq. (8)), respectively. RDR and RCS are equal to v_R and v_G (mol/s) (RDR=v_R, RCS=v_G) for the estimation of $A_R v_R + A_G v_G$.

In this study, the quantitative estimation on the thermodynamic coupling between the reduction reaction of iron oxide and the gasification of graphite was conducted by means of the modification of the experimental apparatus that all the reaction gas could flow in the space between the surfaces of iron oxide and graphite. Furthermore, the ratio of the reduction reaction to the gasification reaction as a function of the distance between the reaction surfaces was examined.

2. Experimental

The experimental apparatus was almost the same as the previous one.[2)] As shown in **Fig. 2**, only the sample holder for making a facing pair was changed to a rectangular crucible (high purity alumina) for flowing the reaction gas into the space between the surfaces of the iron oxide and graphite. In the case of previous setup, the reaction gas passed to the other side (rear side of reaction surface) of sample and the coupling phenomenon might be diluted, although the total reaction degree of reduction and gasification increased because of the increase of reaction surfaces.

However, the modification of sample holder made the experiment difficult owing to the increase in gas linear velocity when the distance between the iron oxide and graphite decreased. Then, the gas velocity was adjusted to two levels, 80 and 10 cm/s for different three distances (0.5, 1.0 and 1.5 mm). **Table 1** shows the details of the present experimental conditions. As a result of modification, the gas flow rate decreased extremely in accordance with the decrease of the distance, which made the quantification of reaction rate difficult by the gas analysis. The total flow rate was from 208 to 625 Ncc/min in the experiment of 80 cm/s, while the one in the 10 cm/s was from 26 to 77 Ncc/min. From these difference of condition, gas analysis became very difficult owing to a small quantity of the reaction and a small amount of produced gas. Then from this reason, the sampling method of the gas was modified as shown in **Fig. 3**. In the experiment of 80 cm/s, the reaction gas was introduced into the gas analyzing tube ($\sim 10^{-4}$ torr) through the VLV (variable leak valve). In this case, the volume from a crucible to VLV was relatively large and the scattering of gas analysis became large when the flow rate of gas decreased. Then, the handmade gas sampling capillary (Fig. 3(b)), which was made by a trial and error for adjusting the total pressure ($\sim 10^{-4}$ torr) of the gas analyzing tube, was set near the outlet of crucible for efficient sampling of produced gas. The capillary was made of quartz and the diameter of a hole in the tip was about 100 μm which was a quite empirical value owing to the function of length of the tip and pressure difference (ΔP). The ΔP will be changed

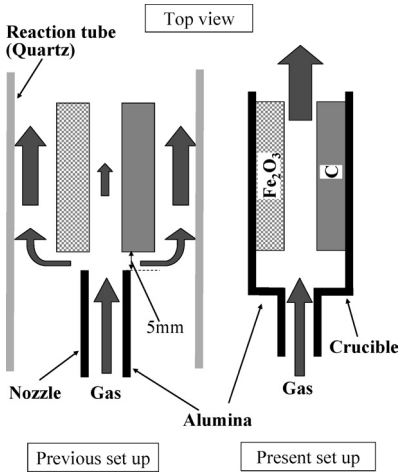

Fig. 2. Comparison of crucible between previous and present experiment.

Table 1. Conditions of flow rate at the different distances of facing pair (Ar–30%CO_2).

Distance (mm)	Total Flow rate (Ncc/min)		Volume between reaction interfaces (cm^3)	10cm/s	
	80cm/s	10cm/s		M^0_{CO2} (mol-CO_2/s)	C^0_{CO2} (mol/s/cm^3)
0.5	208	25.8	0.0524	5.755×10^{-6}	1.098×10^{-4}
1.0	417	51.6	0.1048	1.151×10^{-5}	1.098×10^{-4}
1.5	625	77.4	0.1572	1.727×10^{-5}	1.098×10^{-4}

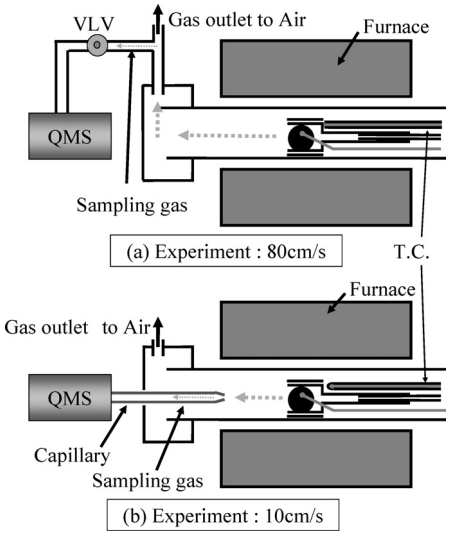

Fig. 3. Improvement of gas sampling method. VLV: variable leak valve, QMS: quatrupole mass spectrometer.

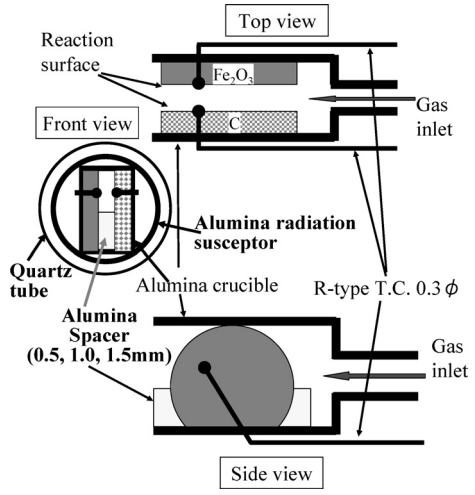

Fig. 4. Alignment of samples and crucible.

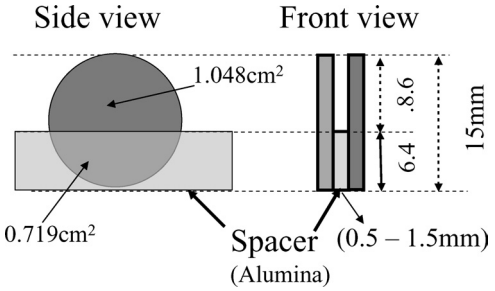

Fig. 5. Dimension of samples and spacer.

by the gas flow rate, gas composition and the temperature. If the tip was located in the high temperature region (>800°C), a softening might occur and the amount of gas passing through the capillary decreased during experiment. Although the present experiment was quite difficult one, the optimum conditions were found and the high accurate analysis could be attained for the experiments of 10 cm/s.

Figure 4 shows the alignment of samples (graphite and hematite) in the alumina crucible which was designed for present purpose. The distances (0.5, 1.0 and 1.5 mm) between two samples were adjusted by the thickness of alumina spacer. The thickness of the hematite and the graphite sample was changed so as to fix the rear surface of each sample to the wall of crucible not to permeate the reaction gas. Finally, alumina cement was used for a complete sealing the rear space. The sample was 15 mm in diameter and the height of spacer was 6.4 mm (**Fig. 5**). Then, the surface areas for the reactions in the hematite and graphite samples were 1.048 cm^2, respectively. The concentration of reaction specie (CO_2) in the space between the hematite and the graphite per unit volume and time, $C^{\circ}_{CO_2}$ (mol/s/cm^3) was exactly same for three different distances (Table 1).

The furnace temperature was controlled by B type thermocouple which was located near the crucible (Fig. 3). Furthermore, the variations of temperatures at both the surfaces of samples were measured by R-type thermocouple (0.3 mmϕ). The positions of thermocouples were shown in Fig. 4. The tip of thermocouple was fixed by alumina cement from the rear side of sample and about 50% of tip surface was exposed to the gas beyond the reaction surface.

As the furnace was Infrared Image furnace, alumina radiation susceptor was located around the crucible, because the shape of crucible was rectangular, which might cause the ununiform temperature distribution (Fig. 4), because the temperature increased by the radiation of IR at the outer surface of the crucible.

The hematite sample was prepared from a reagent grade hematite and compressed into disk shape (15 mmϕ×5 mm) in a mold with 200 kgf/cm^2. Then, the disk shape hematite was sintered in a muffle furnace at 1 200°C for 24 h. The sintered sample was adjusted to the adequate thickness according to the distance between the hematite and graphite. The reaction surface was polished until #1 200 of SiC paper. The ultrasonic cleaning was carried out in an acetone.

Although, in previous study, both of the reaction gases, Ar–30vol%CO_2 and Ar–30vol%CO were used for the initiation of gasification and reduction, respectively, only the Ar–30vol%CO_2 was used in the present study. Heating up rate was 15°C/min from the ambient temperature to 1 000°C and held at 1 000°C for 30 min. The variation of gas composition was continuously monitored by QMS (quadrupole mass spectrometer) and the rates of reactions were calculated after each experiment. The standard gas (40 vol%CO, 20 vol%CO_2 argon balance) was used for calibration of QMS output that was performed before and after experiments, because the condition of QMS (ex. the amount of gas adsorption inside the container (gas analyzing) tube of quadrupole) was changed with time. The precise control of temperature around QMS made the high accurate measurement possible. As the sensitivity of QMS was quite high (≦10 ppm), small amount of reaction can be detected, and the accuracy of measurement was 0.1% for the total flow rate. Then, in this experiment, 0.02–0.07 Ncc/min flow rate(depending on the total flow rate) can be detected, which corresponded to 1.0×10^{-7} (mol/s) as a reduction rate (RDR).

The rate of reduction (RDR) and gasification (RCS) can be obtained by the oxygen balance and carbon balance in the reactant and product gases, respectively. RDR and RCS are equal to v_R and v_G (mol/s) (RDR=v_R, RCS=v_G) for the calculation of $A_R v_R + A_G v_G$, respectively.

Oxygen Balance: rate of reduction

$$\mathrm{RDR\,(mol/s)}=([\mathrm{CO}]_{out}+2[\mathrm{CO_2}]_{out}-[\mathrm{CO}]_{in}-2[\mathrm{CO_2}]_{in})/22\,412/60 \quad \text{.....(7)}$$

Carbon Balance: rate of gasification

$$\mathrm{RCS\,(mol/s)}=([\mathrm{CO}]_{out}+[\mathrm{CO_2}]_{out}-[\mathrm{CO}]_{in}-[\mathrm{CO_2}]_{in})/22\,412/60 \quad \text{.....(8)}$$

Where [CO] and [CO_2] mean the mass flow rate of respective gases in Ncc/min and subscripts 'in' and 'out' mean the inlet and the outlet.

3. Results and Discussions

Figure 6 shows the comparison of results among three distances of facing pair for the linear velocity of gas, 80 cm/s. In the case of 80 cm/s, scattering of data was large and the smoothing of the curves of RDR and RCS (except the data of RDR at 0.5 mm) were carried out. As the reac-

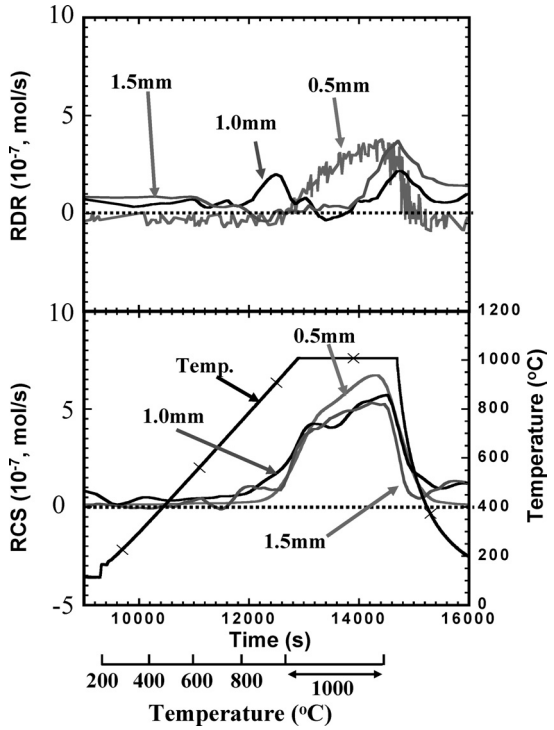

Fig. 6. Comparison of RDR and RCS among three distances (0.5 mm, 1.0 mm and 1.5 mm). (Ar–30%CO_2: 8 0 cm/s, facing pair)

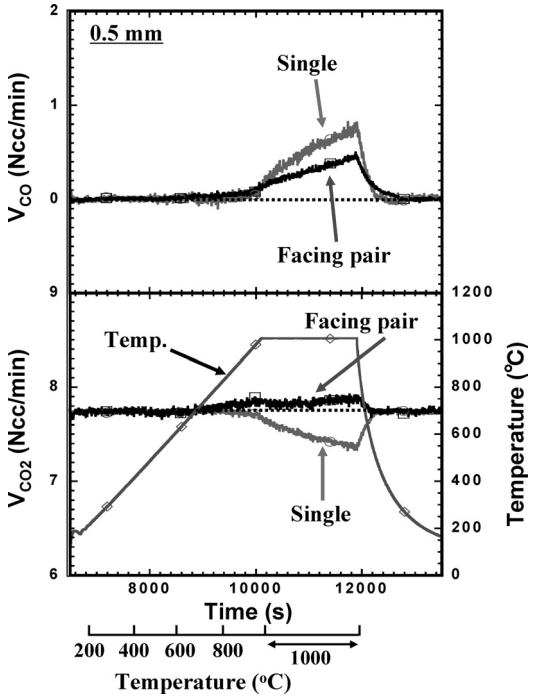

Fig. 7. Variations of CO and CO_2 flow rates with time. (Ar–30%CO_2: 10 cm/s, 0.5 mm, facing pair: hematite–graphite pair, single: graphite–alumina pair)

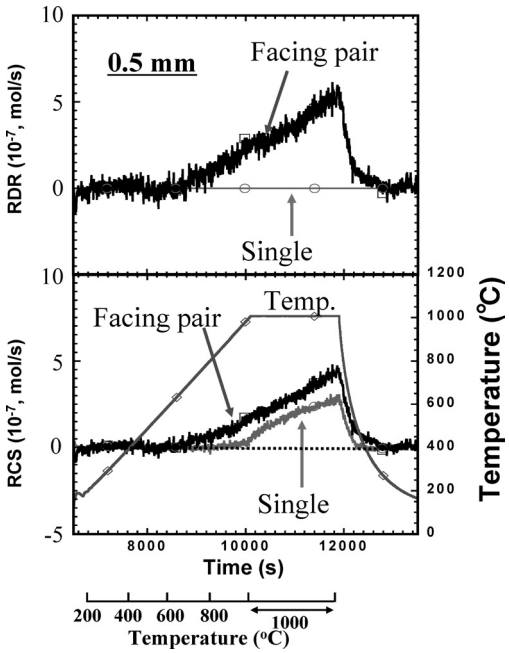

Fig. 8. Variations of RDR and RCS with time. (Ar–30%CO_2: 10 cm/s, 0.5 mm, facing pair: hematite–graphite pair, single: graphite–alumina pair)

tion gas was Ar–30%CO_2, gasification (RCS) was prominent for all distances and could not distinguish the difference of the distance. On the other hand, reduction rate (RDR) was quite unstable and showed relatively small values. In comparison with the previous value,[2] maximum reduction rates for these experimental conditions was almost the same order. However, the profiles were quite unstable and seemed to have no regularity. The order of RCS in previous study[2] was much larger than that in present study, because the reaction gas was flow in the rear surface of the sample and apparent reaction area was larger. The flow rate in the previous study was 500 Ncc/min and the linear velocity at the outlet of the 'gas-inlet' tube was 66 cm/s. However, the actual gas flow rate in the space between the hematite and the graphite would be smaller than that in present study. From these results, the modified experiment was carried out with the linear velocity of 10 cm/s and the quantitative estimation carried out for clarifying the coupling phenomenon.

Figure 7 shows the results of experiment of 10 cm/s on the distance of 0.5 mm for facing pair (hematite-graphite pair) and single graphite (graphite–alumina pair). The total flow rate of reaction gas was 25.8 Ncc/min and the flow rate of CO_2 was 7.74 Ncc/min which was expressed in dotted line (lower part of Fig. 7). The results of single graphite show the simple gasification behavior, that is, the one mole of CO_2 was consumed and two moles of CO produced. While in the case of facing pair, both of the flow rates (CO and CO_2) increased from the initial level, which meant the existence of coupling phenomenon by occurring of the reduction reaction.

Using Eqs. (7) and (8), RDR (rate of reduction) and RCS (rate of gasification) were evaluated and compared in **Fig. 8** using the results of Fig. 7. The gasification rate (RCS) in the single graphite arose from about 950°C, which was relatively high temperature from previous one (900°C) and might be caused by the limited reaction surface area in the present experiment (the reaction in the previous experiment occurred both at rear and front surfaces). The maximum RDR and RCS were about 5×10^{-7} (mol/s) and 4.5×10^{-7} (mol/s), respectively. The starting temperatures of both reactions were almost the same and about 600°C which was the same as previous study.

Figure 9 shows the variations of gases in the experiment

of 1.0 mm distance for the facing pair and the single graphite. In this case, there was no increase of the flow rate of CO_2 in the produced gas, which meant the reaction efficiency, decreased owing to the increase of the distance. **Figure 10** shows the profiles of RDR and RCS curves in 1.0 mm. Because of longer distance, the coupling phenomenon would be diluted and ambiguous, the clear rise of RDR in the range from 600 to 900°C could not be seen (more detail will be mentioned in the later section and Fig. 14). However, the maximum RDR and RCS in 1 000°C increased to 5.7×10^{-7} (mol/s) and 6.5×10^{-7} (mol/s), respectively, in comparison with the one at 0.5 mm.

Figures 11 and **12** show the results of the distance in 1.5 mm. Although the difference from the single graphite became small, the clear arise in RDR and RCS from 600°C were found, which meant the existence of coupling phenomenon at relatively longer distance, 1.5 mm.

In **Figure 13**, the changes of flow rate of gases (CO and

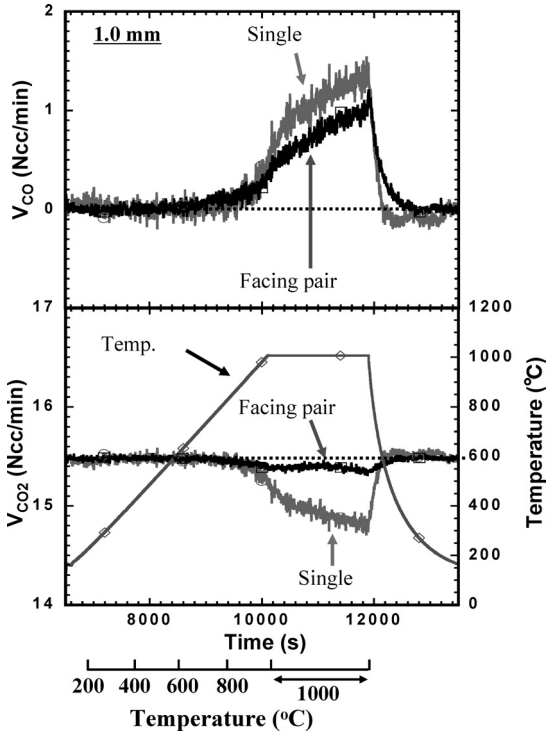

Fig. 9. Variations of CO and CO_2 flow rates with time. (Ar–30%CO_2: 10 cm/s, 1.0 mm, facing pair: hematite–graphite pair, single: graphite–alumina pair)

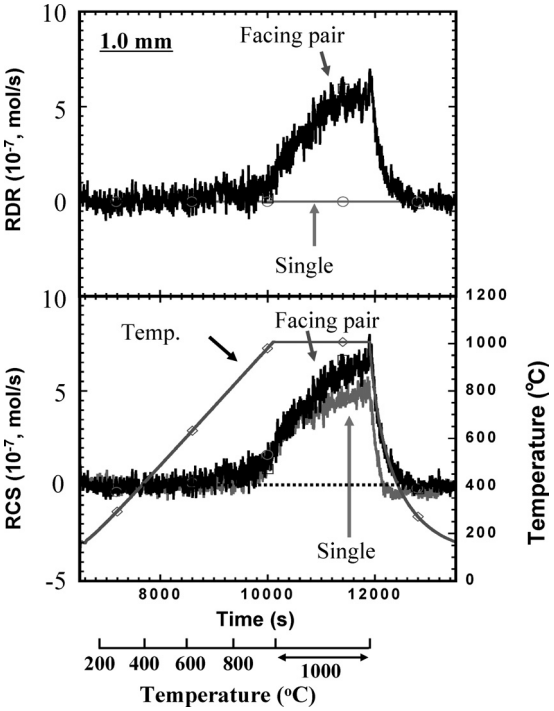

Fig. 10. Variations of RDR and RCS with time. (Ar–30%CO_2: 10 cm/s, 1.0 mm, facing pair: hematite–graphite pair, single: graphite–alumina pair)

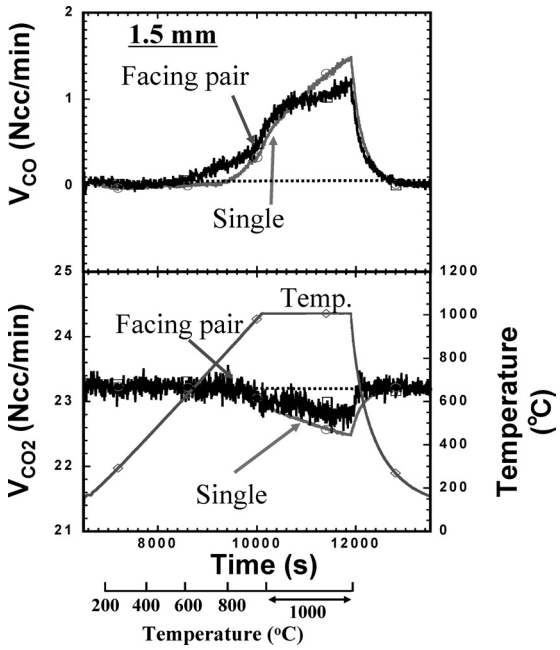

Fig. 11. Variations of CO and CO_2 flow rates with time. (Ar–30%CO_2: 10 cm/s, 1.5 mm, facing pair: hematite–graphite pair, single: graphite–alumina pair)

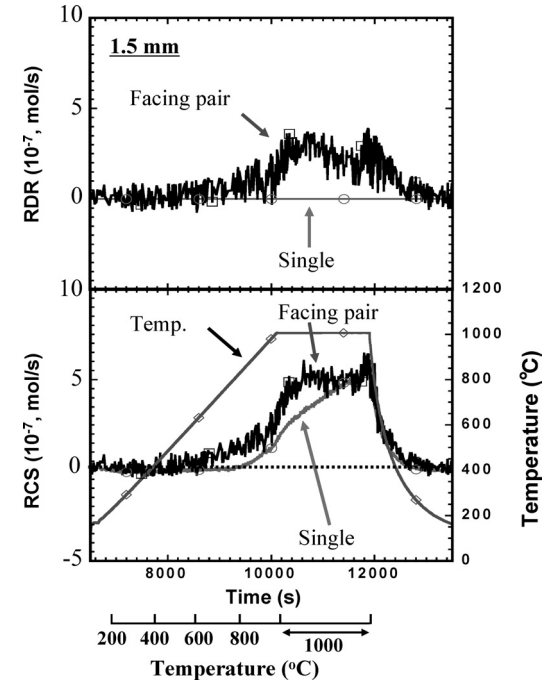

Fig. 12. Variations of RDR and RCS with time. (Ar–30%CO_2: 10 cm/s, 1.5 mm, facing pair: hematite–graphite pair, single: graphite–alumina pair)

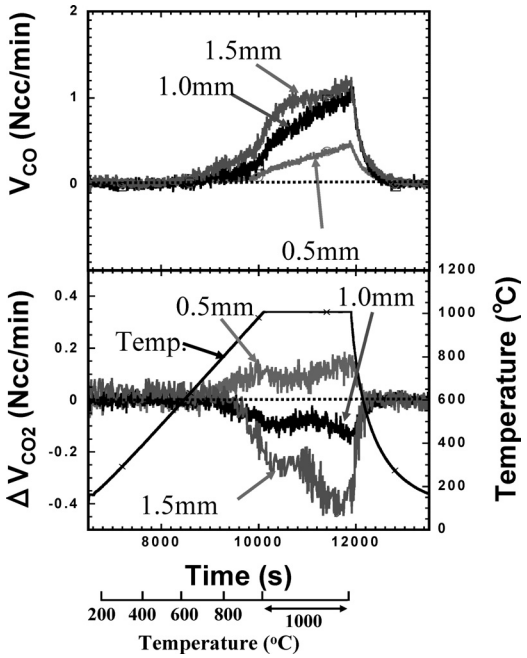

Fig. 13. Comparison of CO_2 and CO flow rates among three distances. (Ar–30%CO_2: 10 cm/s, facing pair: hematite–graphite pair)

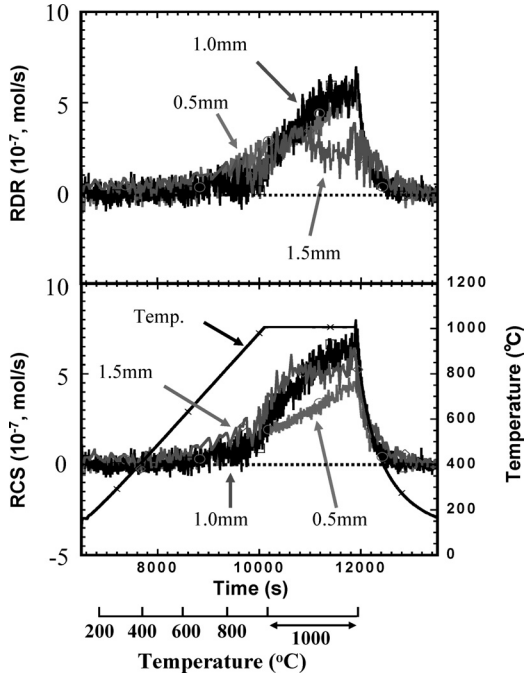

Fig. 14. Comparison of RDR and RCS among three distances. (Ar–30%CO_2: 10 cm/s, facing pair: hematite–graphite pair)

CO_2) in the produced gas were compared in terms of the distance of facing pair. The CO_2 flow rate was changed from positive value (increase) at 0.5 mm to negative (decrease) at 1.0 mm and 1.5 mm. On the other hand, CO gas increased with the distance of facing pair. These results do not reveal the magnitude of coupling phenomenon, but show the intensity of reactions according to the amount of reaction gas (total flow rate of reaction gas increase with the increase of the distance, Table 1) and the extent of reproducibility of CO gas from CO_2. The RDR and RCS were calculated from the gas flow rate in the produced gas using Eqs. (7) and (8) as mentioned above and compared in **Fig. 14**. RCS in the distance of 0.5 mm was lowest among three conditions, while RDR was nearly highest, which meant that coupling phenomenon was largest at the distance of 0.5 mm. Although the starting temperatures of RDR and RCS were ambiguous in the longer distance in 1.0 mm and 1.5 mm (Fig. 10 and Fig. 12), it could be concluded that the starting temperatures of both reactions were about 600°C in Fig. 14.

The variations of $A_R v_R + A_G v_G$ for the different distances were evaluated and shown in **Figs. 15** to **17**. Every $A_R v_R + A_G v_G$ showed a positive value which meant the both of reactions could occur. The necessary condition of coupling reaction was ($A_R v_R < 0$ and $A_G v_G > 0$) and $A_R v_R + A_G v_G > 0$. Since A_R was negative for the inlet gas (A_{Rin}), it could be concluded that the coupling phenomenon should occur from the view point of the inlet gas. As the affinity of the reduction in outlet gas, A_{Rout} was changed to a positive value, the condition of coupling phenomenon was lost until the end of the reaction area in the samples. However, the condition of coupling phenomenon would clearly exist in the part of upstream. The tendencies of $A_R v_R + A_G v_G$ for three distances were almost the same, and the positive values decreased equally from the inlet gas to the outlet one. It would be interesting to note that the reaction rates and the

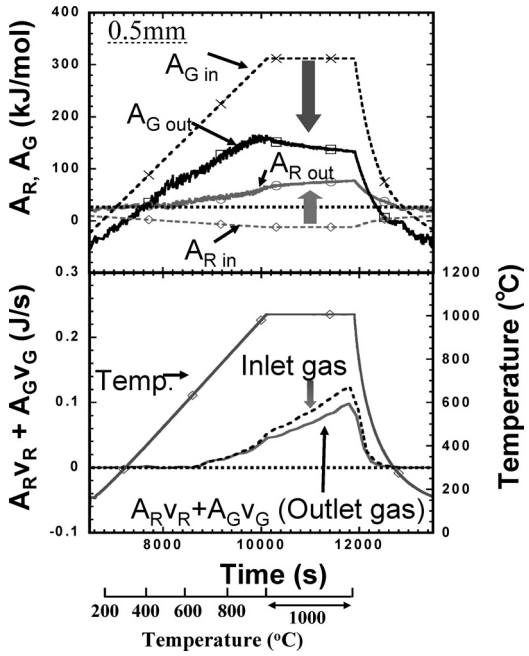

Fig. 15. Variations of A_R, A_G and $A_R v_R + A_G v_G$ with time. (Ar–30%CO_2: 0.5 mm, 10 cm/s, facing pair: hematite–graphite pair)

values of $A_R v_R + A_G v_G$ were not constant in the region of constant temperature (1 000°C). Those values were rapidly increasing when the temperatures were controlled at constant (1 000°C), which meant that those reactions occurring in two reaction surfaces would be a mutual-activated reaction. The results of temperature measurements by the thermocouples at the both surfaces showed that the surface temperatures were already constant.

In this study, reduction reaction (RDR) never occurred without gasification reaction (RCS). Therefore the ratio of

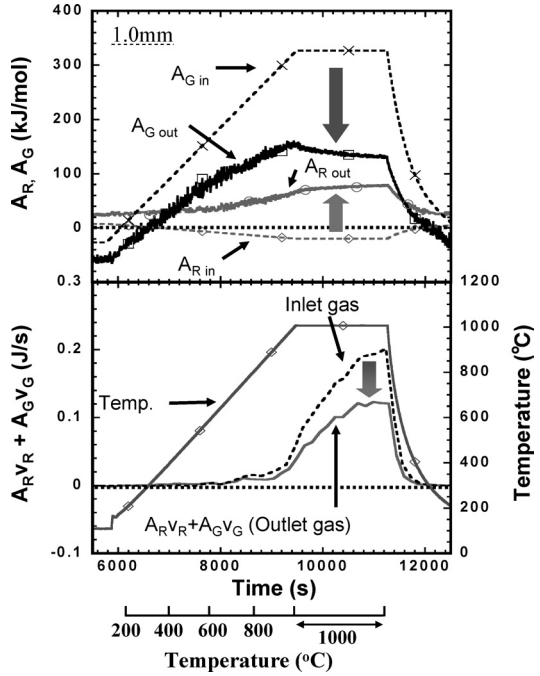

Fig. 16. Variations of A_R, A_G and $A_R v_R + A_G v_G$ with time. (Ar–30%CO_2: 1.0 mm, 10 cm/s, facing pair: hematite–graphite pair)

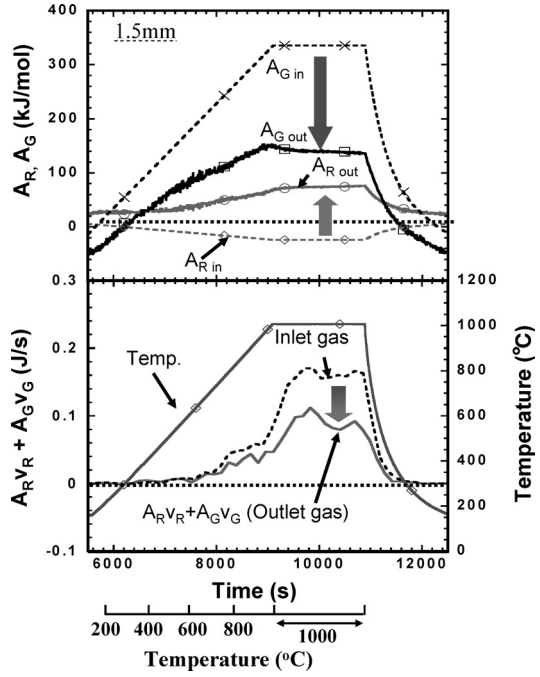

Fig. 17. Variations of A_R, A_G and $A_R v_R + A_G v_G$ with time. (Ar–30%CO_2: 1.5 mm, 10 cm/s, facing pair: hematite–graphite pair)

RDR to RCS means the efficiency of the system. When a equimolar reaction between the reduction (RDR: Eq. (1)) and the gasification (RCS: Eq. (2)) occurs in the system, the plot of RDR *vs.* RCS in experiment will be equal to the line of RCS=RDR. The overall reaction can be written as Eq. (9).

$$Fe_xO_y + C = Fe_xO_{y-1} + CO \quad (RDR/RCS = 1) \text{.....} (9)$$

When the proportion of RDR increased with a higher efficiency, the ultimate line of the ratio would be 2RCS=RDR, which meant that the evolved CO gas through gasification reaction expressed by Eq. (2) was completely utilized in reduction reaction (Eq. (1)). In this case, the overall reaction can be written as Eq. (10).

$$Fe_xO_y + C = Fe_xO_{y-2} + CO_2 \quad (RDR/RCS = 2) \text{.....} (10)$$

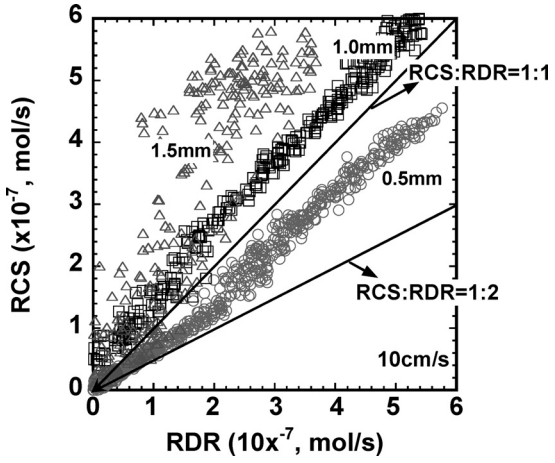

Fig. 18. Plots of RDR (reduction rate) *vs.* RCS (gasification rate) for three distances.

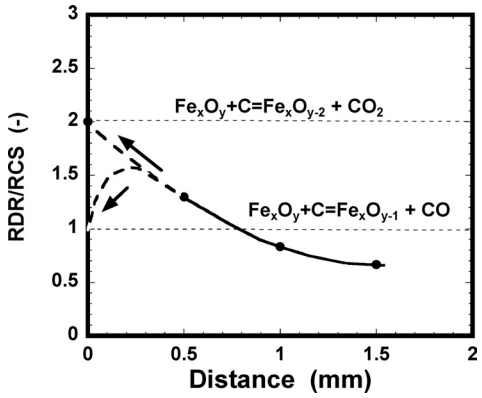

Fig. 19. Variation of RDR/RCS with the distances of facing pair.

These situations are summarized in **Fig. 18**. In the case of longer distances (1.0 mm and 1.5 mm), the plots of RCS *vs.* RDR were located in the left hand side of the line RCS=RCS, which meant that the reaction efficiency in the system was not so high. While the plot in 0.5 mm was located between the lines of RCS=RDR and 2RCS=RDR. Especially, in a region of lower reaction rate than 2×10^{-7} mol/s, which was corresponding to the lower temperature than 900°C, the plot was close to the line of 2RCS=RDR.

In **Fig. 19**, the value of RDR/RCS was plotted to the distance of reaction surface. When the distance of reaction surface decreased from 1.5 to 0.5 mm, the value increased from 0.7 to 1.3. From the extrapolation of the line to a zero of the distance, which is corresponding to the ideal contact between hematite and graphite, the RDR/RCS seems to approach to 2.0. However, this estimation was not coincide with the experimental result of the mixture milling of hematite and graphite, so that the gas composition evolved from the reaction of nano-reactor during the heating-up experiment under an argon atmosphere was only CO gas (RDR/RCS=1), where the ideal contact between the iron

oxide and the graphite would be attained.[5–7] It could not avoid to mention that the nano-level mechanism of CO_2 evolution was not yet clarified when the interfaces closed to a contact. It would be a interesting subject of study in the future, because the efficiency of the reaction system could increase with the concentration of CO_2 evolved.

4. Conclusions

The quantitative estimation of coupling phenomenon between reduction and gasification was carried out with modified experimental setup. All reaction gas (Ar–30%CO_2) could be passed through the space of facing pair of iron oxide (hematite) and graphite. Reduction reaction was promoted by the gasification reaction occurring in the opposite surface. Following results were obtained.

(1) Reduction and gasification for the facing pair of hematite and graphite from 0.5 to 1.5 mm in the distance were occurred from about 600°C, while the gasification reaction for the graphite and alumina pair was occurred from 950°C.

(2) In the shortest distance, 0.5 mm, the CO_2 flow rate increased in the outlet gas, which meant that the reduction reaction was promoted and CO_2 gas reproduced.

(3) The ratio of RDR (reduction rate) to RCS (gasification rate) increased until the distance of 0.5 mm. The value of RDR/RCS seemed to approach to '2' beyond '1' in the case of the shortest distance of 0.5 mm, which meant that the efficiency of the reaction system became a maximum.

Acknowledgement

The present study has been carried out in the research group of 'Project for the innovational ironmaking reaction in new blast furnace at half energy consumption and minimum environmental influences' supported by Special Coordination Founds of the Science and Technology Agency of the Japanese Government (1999–2004). The authors would like to express great appreciation to the member of research group for the valuable discussions.

REFERENCES

1) K. Ishii: *ISIJ Int.*, **44** (2004), 1969.
2) Y. Kashiwaya, M. Kanbe and K. Ishii: *ISIJ Int.*, **41** (2001), 818.
3) De Donder: *Bull. Ac. Roy. Belg. Cl. Sc. (5)*, **7** (1922), 197.
4) M. Chase: JANAF Thermochemical Tables, 4th ed., *J. Phys. Chem. Ref. Data*, (1998).
5) Y. Kashiwaya, H. Suzuki and K. Ishii: *ISIJ Int.*, **44** (2004), 1970.
6) Y. Kashiwaya, H. Suzuki and K. Ishii: *ISIJ Int.*, **44** (2004), 1975.
7) Y. Kashiwaya and K. Ishii: *ISIJ Int.*, **44** (2004), 1981.